International Journal of Nanomedicine

Dovepress
open access to scientific and medical research

Open Access Full Text Article

ORIGINAL RESEARCH

Low-visibility light-intensity laser-triggered release of entrapped calcein from 1,2-bis (tricosa-10,12-diynoyl)-*sn*-glycero-3-phosphocholine liposomes is mediated through a type I photoactivation pathway

International Journal of Nanomedicine downloaded from https://www.dovepress.com/
For personal use only.

This article was published in the following Dove Press journal:
International Journal of Nanomedicine
20 July 2013
Number of times this article has been viewed

Amichai Yavlovich[1,*]
Mathias Viard[1,2,*]
Kshitij Gupta[1,*]
Jessica Sine[1,*]
Mylinh Vu[1]
Robert Blumenthal[1]
Darrell B Tata[3]
Anu Puri[1,*]

[1]Center for Cancer Research Nanobiology Program, National Cancer Institute, Frederick, MD, USA; [2]Basic Science Program, SAIC-Frederick, Inc., Frederick National Laboratory for Cancer Research, Frederick, MD, USA; [3]Centre for Devices and Radiological Health (CDRH)/Office of Science and Engineering Laboratories(OSEL)/ Division of Physics, US Food and Drug Administration, White Oak, MD, USA

*These authors contributed equally to this work

Correspondence: Anu Puri
Membrane Structure and Function Section, Nanobiology Program, Center for Cancer Research, National Cancer Institute – Building 469, Room 216A, Frederick, MD 21702-1201, USA
Tel +1 301 846 5069
Fax +1 301 846 6210
Email puria@mail.nih.gov

Darrell B Tata
US Food and Drug Administration, CDRH/OSEL/Division of Physics, White Oak Campus, White Oak, MD, USA
Tel +1 301 796 2493
Email darayash.Tata@fda.hhs.gov

Abstract: We recently reported on the physical characteristics of photo-triggerable liposomes containing dipalmitoylphosphatidylcholine (DPPC), and 1,2-bis (tricosa-10,12-diynoyl)-*sn*-glycero-3-phosphocholine ($DC_{8,9}PC$) carrying a photo agent as their payload. When exposed to a low-intensity 514 nm wavelength (continuous-wave) laser light, these liposomes were observed to release entrapped calcein green (Cal-G; Ex/Em 490/517 nm) but not calcein blue (Cal-B; Ex/Em 360/460 nm). In this study, we have investigated the mechanism for the 514 nm laser-triggered release of the Cal-G payload using several scavengers that are known specifically to inhibit either type I or type II photoreaction pathways. Liposomes containing DPPC:$DC_{8,9}PC$: distearoylphosphatidylethanolamine (DSPE)-polyethylene glycol (PEG)-2000 (86:10:04 mole ratio) were loaded either with fluorescent (calcein) or nonfluorescent (^{3}H-inulin) aqueous markers. In addition, a non-photo-triggerable formulation (1-palmitoyl-2-oleoyl phosphatidylcholine [POPC]:$DC_{8,9}PC$:DSPE-PEG2000) was also studied with the same payloads. The 514 nm wavelength laser exposure on photo-triggerable liposomes resulted in the release of Cal-G but not that of Cal-B or ^{3}H-inulin, suggesting an involvement of a photoactivated state of Cal-G due to the 514 nm laser exposure. Upon 514 nm laser exposures, substantial hydrogen peroxide (H_2O_2, ≈100 μM) levels were detected from only the Cal-G loaded photo-triggerable liposomes but not from Cal-B-loaded liposomes (≤10 μM H_2O_2). The Cal-G release from photo-triggerable liposomes was found to be significantly inhibited by ascorbic acid (AA), resulting in a 70%–80% reduction in Cal-G release. The extent of AA-mediated inhibition of Cal-G release from the liposomes also correlated with the consumption of AA. No AA consumption was detected in the 514 nm laser-exposed Cal B-loaded liposomes, thus confirming a role of photoactivation of Cal-G in liposome destabilization. Inclusion of 100 mM $K_3Fe(CN)_6$ (a blocker of electron transfer) in the liposomes substantially inhibited Cal-G release, whereas inclusion of 10 mM sodium azide (a blocker of singlet oxygen of type II photoreaction) in the liposomes failed to block 514 nm laser-triggered Cal-G release. Taken together, we conclude that low-intensity 514 nm laser-triggered release of Cal-G from photo-triggerable liposomes involves the type I photoreaction pathway.

Keywords: visible laser-triggered payload release, photo-agents, photopolymerizable phospholipids, photodynamic actions, reactive oxygen species

Introduction

In the field of cancer nanomedicine, liposomes have long been sought as nanocarriers to improve drug delivery and efficacy through an increase in local drug concentration

© 2013 Yavlovich et al, publisher and licensee Dove Medical Press Ltd. This is an Open Access article which permits unrestricted noncommercial use, provided the original work is properly cited.

within targeted tissue.[1–4] Several studies have described the synthesis and properties of photoreactive molecules (primarily lipids) designed to enhance localized drug delivery (triggered release) upon activation by a suitable light source (photo-triggering).[5–12] Photo-triggering typically involves activation of the photosensitive molecules, causing a perturbation (destabilization) of the liposome membrane.[7,13,14] Release mechanisms of liposome-entrapped drugs and pharmaceuticals are generally based on localized membrane destabilization due to structural changes in fatty acid chains[5,7,11,15] (for further information on the mechanism[s] of photo-triggering of the lipid bilayers for enhanced drug delivery, readers are referred to comprehensive reviews).[9,11,16–18] However, the mechanistic role of photo-activated liposome-encapsulated molecules (drugs or fluorescent solutes) in the release has not been addressed. Upon photo-agent activation through visible wavelength photon absorption, photo-agents that possess a quantum metastable state could exert significant oxidative stress through extensive generation of singlet oxygen $^1O_2$ (energy-transfer pathway known as type II mechanistic pathway), as well as through the generation of O_2^- and H_2O_2 (electron-transfer pathway known as type I pathway).[19]

In our previous studies, we have described photo-triggerable liposome formulations, which contain a saturated lipid as the matrix component (dipalmitoylphosphatidylcholine [DPPC]) and a photopolymerizable diacetylenic lipid (1,2-bis[tricosa-10,12-diynoyl]-*sn*-glycero-3-phosphocholine [$DC_{8,9}PC$]). Our liposome design also includes a polyethylene glycolated (PEGylated) lipid for future localized drug-delivery applications in cancer treatments.[10,14] The aqueous compartment of our formulated liposomes could be loaded with desired molecules of choice such as the photo-agent calcein or an anticancer agent such as doxorubicin.[14] The matrix lipid (such as DPPC) of choice was found to be important for light-triggered release of payload content, as other investigated matrix lipids (such as egg PC or 1-palmitoyl-2-oleoyl phosphatidylcholine [POPC]) did not result in a photo-triggerable release (see Figure 1A). We have analyzed these findings in detail, and have attributed the influence of the lipid type to lipid packing.[20] In addition we made the observation that the 514 nm wavelength laser-triggered release of the payload content from our photo-triggerable formulation was dependent on the optical properties of payload molecules.[14]

We have summarized the design and utility of photo-triggerable liposomes in Figure 1A. The lipid structures used in these studies are shown in Figure 1B. Liposomes that were selectively prepared from DPPC and $DC_{8,9}PC$ (formulation I, Table 1 and Figure 1A) were photo-triggerable.[10] Our formulated liposomes were found to release their payload (either calcein or doxorubicin) upon either an ultraviolet (UV) (254 nm) or to a green (514 nm) laser light exposure.[14] The DPPC matrix lipid properties were found to play a critical role in the observed release of these two payloads.[20,10] By contrast, formulations that contained POPC (as the matrix lipid) with $DC_{8,9}PC$ (Figure 1A) did not release the two payloads under identical light-exposure parameters. Liposomes containing DPPC as matrix lipids are referred to here as "photo-triggerable formulations," whereas liposomes containing POPC as matrix lipids are referred to as "nonphoto-triggerable formulations." These vast differences in the level of release of the payload from the two differently formulated liposomes were attributed to phase separation of the $DC_{8,9}PC$ clusters within the DPPC matrix (as shown in Figure 1A), but not within the POPC matrix. This deduction is made through our experimental findings using lipid monolayers and molecular dynamic-simulation studies.[20] Interestingly, the UV-mediated release of the payload in formulations containing DPPC as the matrix lipid (Figure 1A) was not dependent on the properties of the payload molecules. In contrast, the green laser light-mediated release was found to occur only from DPPC:$DC_{8,9}PC$ liposomes (formulation I, Table 1 and Figure 1A) that contained either calcein green (Cal-G) or doxorubicin as the entrapped photo-agent. Photo-triggerable formulation with calcein blue (Cal-B) as the payload failed to promote solute release upon treatment with 514 nm green laser (Figure 1A).

In this communication, we investigate the mechanistic pathways for the 514 nm laser-mediated Cal-G release mechanism(s). Based on our findings of substantial measured levels of H_2O_2 and selective inhibition of Cal-G release by ascorbic acid (AA) and $K_3Fe(CN)_6$, but not that by NaN_3, we conclude that the 514 nm laser-triggered release of entrapped Cal-G from our formulated liposomes depends on a photoactivated state of Cal-G, which utilizes the type I photoactivation-reaction pathway. Understanding of the light-triggered release mechanisms is highly advantageous for the suitable design of future nanodelivery systems in biology and medical applications.

Materials and methods

Materials

Phospholipids were purchased from Avanti Polar Lipids (Alabaster, AL, USA). Calcein and nonradioactive inulin was purchased from Sigma-Aldrich (St Louis, MO, USA). Sepharose CL-6B was purchased from GE Healthcare (Pittsburgh, PA, USA). ^{3}H-inulin (inulin-methoxy [methoxy-^{3}H, specific activity: 322 mCi/g]) was bought from

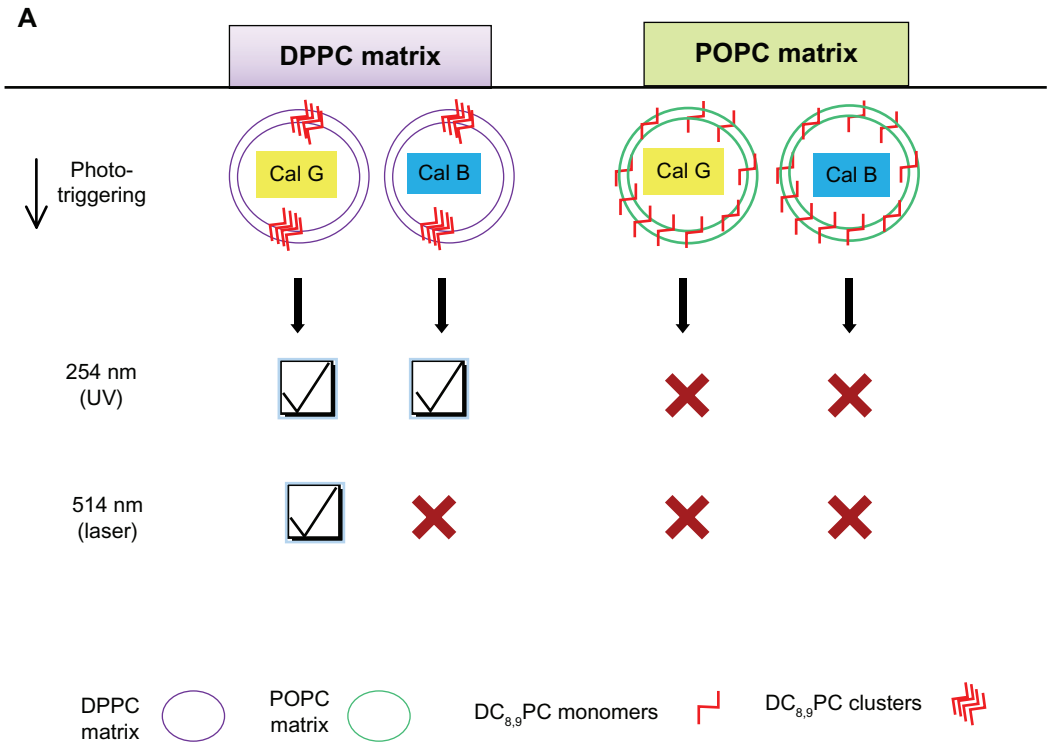

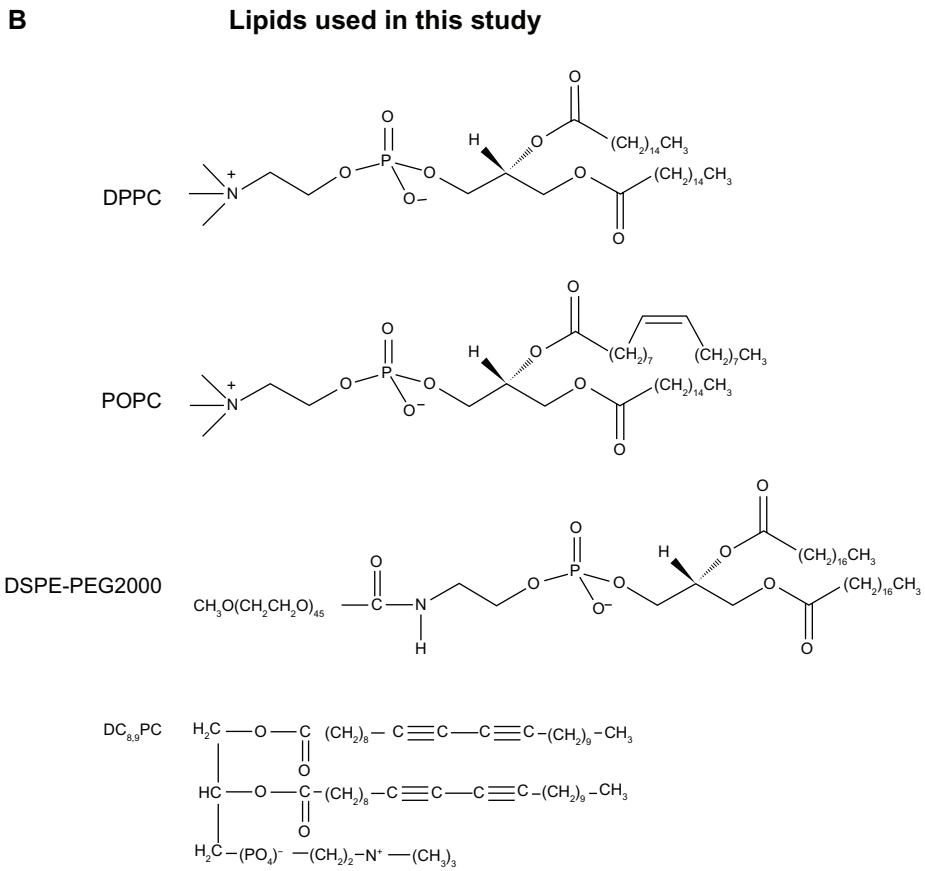

Figure 1 (**A**) Criteria of light-triggered solute release from 1,2-bis (tricosa-10,12-diynoyl)-*sn*-glycero-3-phosphocholine ($DC_{8,9}PC$) liposome formulations. Light sensitivity of liposomes containing the $DC_{8,9}PC$ (red) with either dipalmitoylphosphatidylcholine (DPPC; purple) or 1-palmitoyl-2-oleoyl phosphatidylcholine (POPC; green) are shown. $DC_{8,9}PC$ is clustered in DPPC matrix but relatively homogeneously dispersed in POPC (as shown). Entrapped molecules are either calcein green (Cal-G) or calcein blue (Cal-B). The formulations containing DPPC as the matrix lipid are sensitive to light treatments resulting in release of entrapped solutes (shown by √). Formulations containing POPC are not sensitive to light treatments and hence do not release entrapped solutes (indicated by X). Treatments with 254 nm (ultraviolet [UV]) promote solute release independent of the properties of entrapped solute. Treatments with 514 nm laser, however, require Cal-G as the entrapped solute. (**B**) The lipids used in this study.
Abbreviation: DSPE-PEG2000, 1,2-distearoyl-*sn*-glycero-3 phosphoethanolamine-*N*-(methoxy[PEG]-2000 [ammonium salt]).

Table 1 Liposome formulation reference table

Liposome formulations	Lipid	Ratio	Entrapped marker	Reference to figure number
I	DPPC:$DC_{8,9}PC$	86:10	Calcein green	Figures 2, 4A, B and 5
II	DPPC:$DC_{8,9}PC$	86:10	Calcein blue	Figures 4A and 5
III	DPPC:$DC_{8,9}PC$	86:10	Inulin	Figure 3
IV	DPPC:$DC_{8,9}PC$	86:10	Inulin and calcein	Figure 3

Note: *All formulations contain 4 mol% DSPE-PEG2000.
Abbreviations: DPPC, dipalmitoylphosphatidylcholine; $DC_{8,9}PC$, 1,2-bis (tricosa-10,12-diynoyl)-*sn*-glycero-3-phosphocholine; DSPE-PEG2000, 1,2-distearoyl-sn-glycero-3 phosphoethanolamine-*N*-(methoxy[PEG]-2000 [ammonium salt]).

PerkinElmer (Santa Clara, CA, USA). All materials and buffers were of reagent grade.

Formation of liposomes

The following lipids were used at various ratios and/or combinations to prepare liposomes: DPPC, $DC_{8,9}PC$, and 1,2-distearoyl-*sn*-glycero-3 phosphoethanolamine-*N*-(methoxy[PEG]-2000 [ammonium salt]) (DSPE-PEG2000). The formulations used in this study are shown in Table 1. Liposomes were prepared using probe sonication essentially as described.[10]

Encapsulation of calcein and ^{3}H-inulin in liposomes

Encapsulation of Cal-G or Cal-B

To encapsulate calcein, the lipid film was reconstituted in HEPES (4-[2-hydroxyethyl]-1-piperazineethanesulfonic acid) buffer (pH 7.5) containing a self-quenched concentration of calcein (0.1 M). Sonicated vesicles were formed by sonication at 4°C for 5–10 minutes (1-minute pulses and 1-minute rest) using a Probe Sonicator (W-375; Heat Systems Ultrasonics, New York, NY, USA). The samples were centrifuged to remove any titanium particles and larger aggregates. Solute-loaded liposomes were separated from unentrapped Cal-G or Cal-B using a size-exclusion gel chromatography column (Sepharose CL-6B, 1 × 40 cm, 40 mL bed volume; GE Healthcare). Eluted liposomes were collected, liposome-rich fractions were pooled, and total lipid levels were determined by measuring inorganic phosphorus (Pi) as described.[21] Liposomes were filtered through a 0.45 μm filter (Millex-HV 0.45 μm filter unit; Millipore, Billerica, MA, USA). Calcein loading into liposomes was determined by examining fluorescence before and after addition of Triton X-100 (0.02% final concentration). Fluorescence was measured using a fluorescent microplate reader (SpectraMax M2; Molecular Devices, Sunnyvale, CA, USA). Filter settings (Ex/Em) of 490/517 nm and 360/460 nm were used for Cal-G and Cal-B, respectively.

Inulin encapsulation

Cold inulin was solubilized in phosphate-buffered saline (PBS; pH 6.6) at a concentration of 1% weight by volume. Inulin was incubated for 2 hours at 55°C, and subsequently the solution was kept at room temperature to allow sedimentation of any insoluble material. The clear supernatant was used further. ^{3}H-inulin was reconstituted in MilliQ water (Millipore) at a concentration of 1 μCi/μL.

The lipid film (10 mg, Table 1, formulation III) was hydrated with 50 μCi of ^{3}H-inulin and 0.5 mL of cold inulin. The lipid suspension was kept at 50°C, above the phase-transition temperatures of DPPC and $DC_{8,9}PC$ (41°C and 44°C, respectively) for 10 minutes in a water bath, vortexed intermittently, and allowed to cool at room temperature for 10–20 minutes. This procedure was repeated twice to ensure homogeneous lipid dispersion, and the samples were sonicated as described above. The sonicated liposomes were eluted through the Sepharose CL-6B column preequilibrated with PBS (pH 6.6) to separate unentrapped inulin from inulin-loaded liposomes. Fractions of 1.0 mL were collected, and 0.1 mL from each fraction was analyzed for ^{3}H-inulin using 10 mL of scintillation fluid (Ecoscint A; National Diagnostics, Atlanta, GA, USA) in a scintillation counter (LS6500; Beckman Coulter, Brea, CA, USA). Liposomes typically eluted in fraction 10–12 and were pooled for further experiments. Encapsulation efficiency of ^{3}H-inulin was ≈5% under the experimental conditions used here. Inulin was also coencapsulated with calcein (25 mM) for some experiments (Table 1, formulation IV).

Photo-triggering

Release of entrapped fluorescent molecules from liposomes (typically containing ≈1.5 nmol Pi/mL) after exposure to 254 nm (UV) or 514 nm (visible light) treatments was evaluated.[10,14] Light exposures were performed as described below.

Light treatment

For 254 nm UV treatment, liposomes were placed in a 96-well plate and irradiated using a UV lamp (short-wave assembly 115 V, 60 Hz; UVP, Upland, CA, USA) at a distance of 1 inch at room temperature for 0–45 minutes. For inulin release, samples were treated in quadruplicate and pooled together for monitoring the ^{3}H-inulin release (see below).

Visible-light treatment of liposomes was done using a multiline-mode argon laser (488/514 nm; Lexel Laser, Fremont, CA, USA). The liposomes were placed in a precooled Eppendorf tube and irradiated horizontally with a focused beam intensity of 166 mW/cm^2 with 0- to 10-minute laser-exposure durations.[22] For inulin release, samples were treated in quadruplicate and pooled together for monitoring the ^{3}H-inulin release (see ^{3}H-inulin release section below).

Measurements of release of contents

Calcein release

Calcein release was measured using a fluorescent microplate reader. Calcein release of 100% was obtained after addition of Triton X-100 (0.02%, final concentration).

^{3}H-inulin release

After treatments with UV or laser, the samples were pooled and then fractionated on the Sepharose CL-6B column pre-equilibrated with PBS. Untreated (control) liposomes were also fractionated in identical fashion. Fractions of 1.0 mL were collected and analyzed for ^{3}H-inulin, as previously mentioned. The liposomes coencapsulated with calcein and inulin were analyzed for radioactivity and fluorescence, as previously mentioned.

Effect of inhibitors on photo-triggering

AA was added to the liposomes, and the samples were incubated at room temperature for 24 hours. The samples were exposed to 514 nm laser, and release of contents was measured, as previously mentioned.

To examine the effect of NaN_3 or $K_3Fe(CN)_6$ on light-triggered calcein release from liposomes, these agents (NaN_3 [10 mM] or $K_3Fe[CN]_6$ [100 mM]) were coencapsulated with calcein during the preparation of liposomes. For $K_3Fe(CN)_6$ coencapsulation, we used DPPC:$DC_{8,9}$PC:DSPE-PEG2000 (88:10:02 mol ratio). Control liposomes were prepared without the inhibitors. Unincorporated solutes were removed and calcein release upon photo-triggering was conducted, as previously mentioned. The percentage solute release was monitored. To rule out any direct effect of $K_3Fe(CN)_6$ on Cal-G fluorescence, we assayed Cal-G fluorescence (5 μM) in the absence or presence of $K_3Fe(CN)_6$ at concentrations ranging from 0 μM to 1 mM. We did not observe any effect on Cal-G fluorescence upon addition of $K_3Fe(CN)_6$ (data not shown).

Measurement of H_2O_2 content in laser-treated samples

The activation of the photo-agent calcein upon laser treatment was evaluated by monitoring the production of H_2O_2 in the samples. Liposomes were laser-irradiated (514 nm, 5 minutes) and filtered to separate liposomes from the filtration (released calcein in the solution), followed by measurement of H_2O_2 concentration in the pellets. We used an assay based on the ability of H_2O_2 to convert Amplex red to resorufin (Ex/Em 535/590 nm) using the Amplex Red Enzyme Assay kit (Life Technologies, Carlsbad, CA, USA).

The Amplex red reagent in the presence of horseradish peroxidase was utilized in order to quantify the levels of H_2O_2. The basis of this assay is straightforward. The Amplex red by itself has no absorption at 535 nm; however, its oxidation product, resorufin, is highly absorbent at 535 nm. Amplex red by itself does not become oxidized into resorufin; however, in the presence of a peroxidase such as horseradish peroxidase, Amplex red reacts with H_2O_2 in a 1:1 stoichiometry to yield resorufin. The final resorufin product has minimal absorption below 500 nm and no absorption beyond 625 nm. It has a single absorption peak at 571 nm. H_2O_2 quantitation was done through the absorbance of resorufin at 535 nm in transparent 96-well PerkinElmer ViewPlate 96F within a PerkinElmer Victor^3 1420 multilabel counter plate reader. The H_2O_2 calibration curve from known concentrations of H_2O_2 was measured in the same 96-well plate, which also contained the laser-treated samples for H_2O_2 analyses. The Amplex red assay can spectroscopically resolve down to an H_2O_2 concentration of 100 nM.

To monitor the effect of addition of H_2O_2 (in the absence of laser treatment), liposomes (160 μL) were placed in a 96-well microplate, and H_2O_2 was added at various concentrations (0–5 mM). Incubations were continued either at room temperature (25°C) or 37°C for 0–18 hours. Volumes were adjusted with HEPES-buffered saline in order to maintain consistent dilutions across all samples. Calcein release was determined as previously described.

Results and discussion

It is well established that UV exposures lead to intermolecular photo-cross-linking between $DC_{8,9}$PC monomers, resulting in the formation of $DC_{8,9}$ PC polymers.[14,23–27] The photo-cross-linking of $DC_{8,9}$PC results in change in chromogenic properties of the polymer, often judged by appearance of red/blue color in the samples. UV-triggered payload release from our photo-triggerable formulation is a consequence of $DC_{8,9}$PC polymerization,[10,20] based on detection of photo- cross-linked $DC_{8,9}$PC monomers[10,20] (accompanied by appearance of red and spectral shifts) and significant changes in the morphology of UV-treated liposomes (cryo-electron microscopy, unpublished observations). Surprisingly, we did not see any

evidence of photo-cross-linking in 514 nm green laser-treated liposomes (formulation I), though Cal-G release was clearly evident (Figure 2). Therefore, the mechanism(s) by which the green laser-light exposure promoted payload release from formulation I are not known and became the focus of this investigation, and motivated us to further undertake this study in understanding the mechanism(s) responsible in the Cal-G release from our formulation I.

Two possible pathways were hypothesized: direct photo-damage to the lipid molecules by green laser, causing a perturbation in the lipid bilayer or interactions of green light activated photo-agents, and/or resulting reactive oxygen species (ROS) with the lipid bilayer leading to liposome destabilization. We reasoned that if direct light-induced lipid damage occurred due to the green laser exposure, then formulation II (loaded with Cal-B)[14] and III (loaded with inulin) would also exhibit payload release (Figure 3). Our results revealed that the green laser is incapable of releasing the payloads from our formulated II (previous studies[14]) and III liposomes. The green laser-triggered release of payload was only observed from formulation I or IV, which were loaded with Cal-G. Therefore, we endeavored to examine the photoactivated state of liposome-encapsulated Cal-G for the observed content release from our photo-triggerable formulation I. We examined the effects of various free radical scavengers specific for photoreaction type I and II pathways in order to gain insight into the potential ROS involved in the processes leading to the release of the payload content. The results obtained from these studies are presented and discussed here.

Calcein green as entrapped photo-agent is essential for 514 nm laser-induced release from DPPC:$DC_{8,9}PC$ liposomes

Liposome formulations containing DPPC:$DC_{8,9}PC$ were prepared with entrapped photo-agent Cal-G. The liposomes were treated with either a 514 nm laser (up to 10 minutes) or with a 254 nm UV light source (40 minutes). Control samples were not treated with light (Figure 2). It is clear from the images that a shift in chromogenic properties occurred upon UV but not laser treatment. However, the Cal-G release occurred upon 254 or 514 nm treatment (Figure 2, bar graph), consistent with our previous findings.[14] These data allude to the fact that properties of entrapped molecules play a role in 514 nm laser but not in the 254 nm (UV) mediated release of contents from our photo-triggerable formulations.

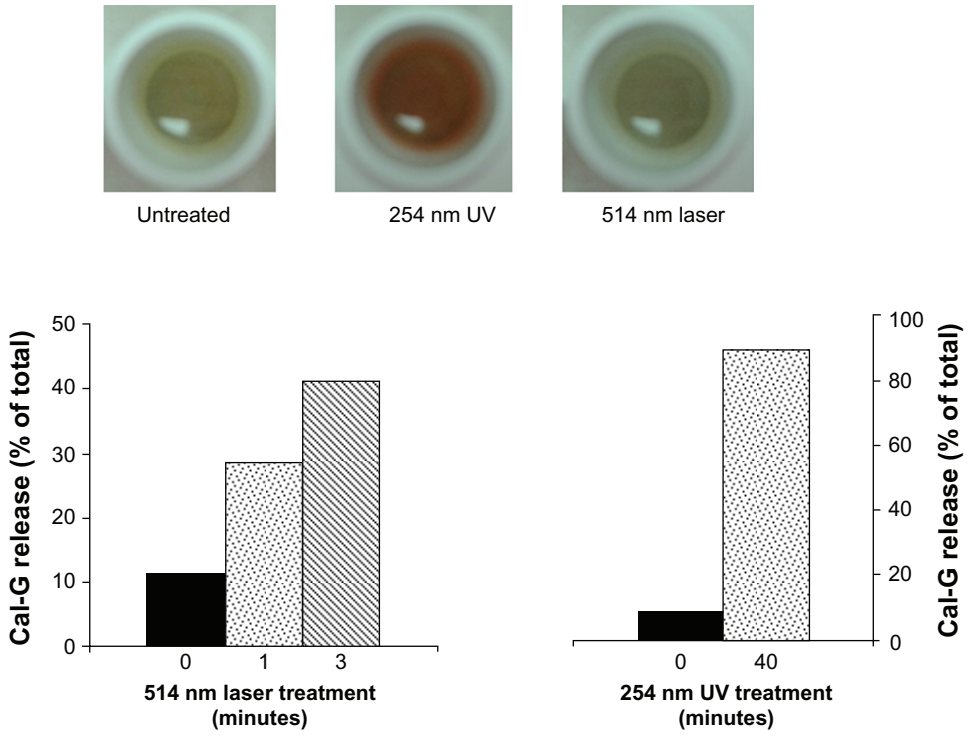

Figure 2 Effect of light treatment on calcein green (Cal-G)-loaded dipalmitoylphosphatidylcholine (DPPC):1,2-bis (tricosa-10,12-diynoyl)-*sn*-glycero-3-phosphocholine ($DC_{8,9}PC$) liposomes. Liposomes (100 μL, formulation I, Table 1) were placed in wells of a 96-well plate for polymerization assay. The samples were either treated with 254 nm ultraviolet (UV; 40 minutes) or 514 nm laser (10 minutes) as indicated. Untreated liposomes served as a control. Following treatments, the wells were photographed using a color camera and images are shown as indicated. For Cal-G release, liposomes were treated with either 254 nm UV or 514 nm laser at indicated times. Fluorescence was measured at Ex/Em 490/517 nm and percentage release was calculated (Materials and methods section).

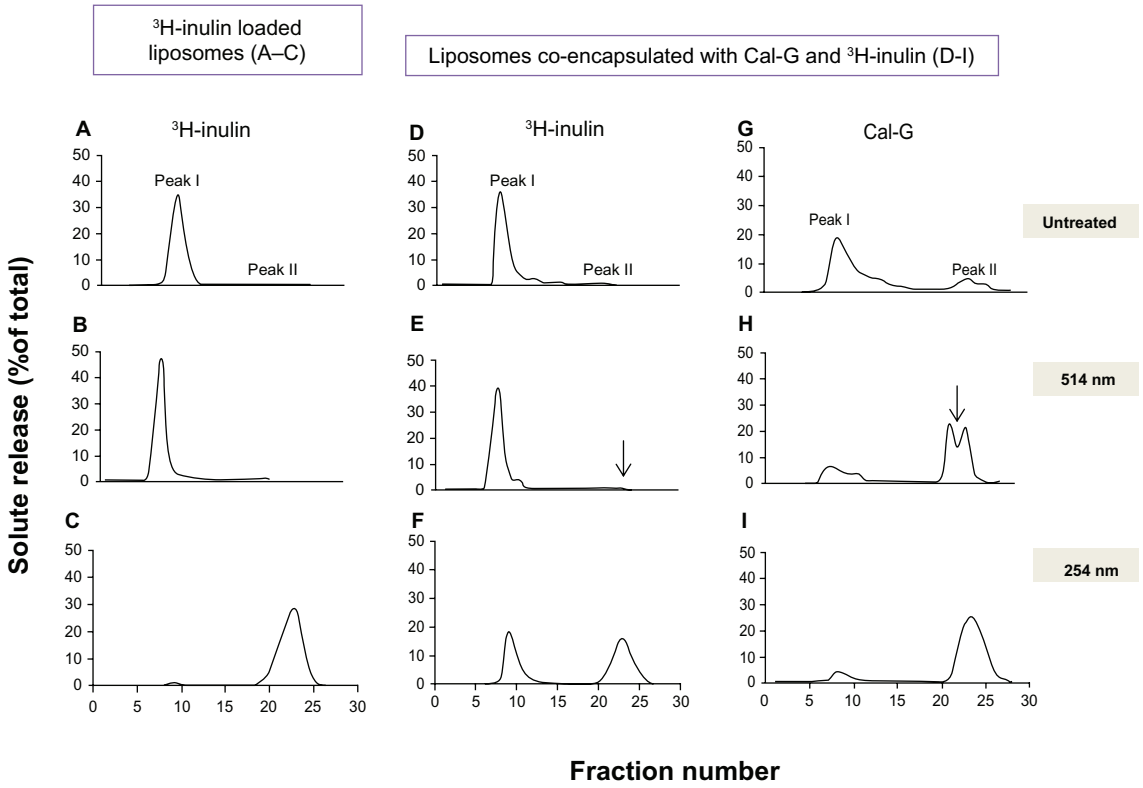

Figure 3 Effect of light treatment on release of inulin from liposomes. Liposomes were prepared either with encapsulated ^{3}H-inulin only (formulation III, Table 1) or coencapsulated with calcein green (Cal-G) and ^{3}H-inulin (formulation IV, Table 1) and treated with either 514 nm laser (10 minutes, **B**, **E** and **H**) or 254 nm (45 minutes, **C**, **F** and **I**). Untreated liposomes were used as controls (**A**, **D** and **G**). Released solutes were separated from liposome-encapsulated solutes by fractionation of the samples on Sepharose CL-6B column collecting 1.0 mL fractions (×30). The fractions were analyzed for radioactivity and fluorescence (Materials and methods section). The values are expressed as percent solute present in each fraction taking the total radioactivity or fluorescence in all 30 fractions as 100%.
Notes: Peak I, liposomal solutes; peak II, free solutes. The data are reproducible from two independent experiments.

To deepen our understanding of the mechanistic role of photo-agents resulting in the observed release from DPPC:$DC_{8,9}$PC liposomes, we prepared DPPC:$DC_{8,9}$PC liposomes containing a nonfluorescent entrapped payload: inulin (formulation III) or inulin/Cal-G coencapsulated liposomes (formulation IV). Trace amounts of radioactive inulin (^{3}H-inulin) were also included to monitor the payload release in these formulations (Table 1 and Figure 3).[28–30] Details of inulin encapsulation and release are provided in the Materials and methods section. In our first series of experiments, we examined release of entrapped inulin from formulation III that contained only nonfluorescent marker, inulin following treatments with either 254 or 514 nm wavelength light. Results are presented in Figure 3A–C. Light-treatment conditions are shown on the far right of the figure. Values are presented as percentage ^{3}H-inulin associated with liposomes (peak I) and free inulin (peak II). A near-complete release of inulin was observed in 254 nm-exposed DPPC:$DC_{8,9}$PC liposomes (Figure 3C). In contrast, we did not observe inulin release from the DPPC:$DC_{8,9}$PC liposomes exposed to the 514 nm laser light (Figure 3B) compared to the unexposed condition (Figure 3A). Evidently, the presence of Cal-G in the payload of the DPPC:$DC_{8,9}$PC liposomes appears essential for the 514 nm-mediated release.

In the next series of experiments, we coencapsulated Cal-G and inulin in the DPPC:$DC_{8,9}$PC liposomes (Table 1, formulation IV), and treated with either 254 or 514 nm green laser. The results are shown in Figure 3D–I. Upon 254 nm treatment, both inulin (Figure 3F) and Cal-G (Figure 3I) were released, as expected. In contrast, when formulation IV was treated with the 514 nm green laser, only Cal-G was released (Figure 3H). We did not see any free ^{3}H-inulin associated with peak II (Figure 3E). The selective release of Cal-G from Cal-G/inulin-loaded liposomes in response to 514 nm laser is probably due to the limited diffusion of inulin in comparison to Cal-G (molecular weight of Cal-G ~623 g/mol and that of inulin ~5000 g/mol) through the presumed photo-induced membrane perturbations. Continued incubations of 514 nm green laser light-treated formulation IV (16 hours at 37°C) did not result in any significant leakage of inulin (data not shown), indicating that the nature and characteristics of 514 nm laser-induced membrane perturbations are very distinct from the

254 nm-treated samples. This area of research is subject to further investigations. Taken together, the data presented in Figure 3 confirm that 514 nm wavelength laser-triggered release of contents from our formulations requires a matching wavelength-specific photoactivator.

Effect of photoactivation inhibitors on 514 nm laser-triggered release of Cal-G

Light-mediated biochemical effect from activated photo-agents typically occurs via type I or type II pathways,[19] and agents that block these pathways have been reported in the literature. In this study, we used three scavengers: AA, NaN_3, and $K_3Fe(CN)_6$. NaN_3 is known in the literature to inhibit singlet oxygen (type II) reactions, AA is known to inhibit both type I and type II pathways, and $K_3Fe(CN)_6$ is known to inhibit electron-transfer reactions (type I). Results from these scavenger studies are presented below.

Ascorbic acid, an oxygen radical scavenger, inhibits 514 nm laser-triggered Cal-G release

Unsaturated lipids are known to undergo lipid peroxidation, which can lead to significant effects (mostly detrimental) in various biological processes.[31–34] Typically, lipid peroxidation is a consequence of generation of ROS, including free radicals, hydroxyl ions, and hydrogen peroxide, as well as potential electron transfer to/from the unsaturated bonds (such as olefins).[33–35] Our nontriggerable liposomes (Figure 1) contain POPC that contains unsaturated bonds (Figure 1B) in addition to $DC_{8,9}PC$, which contains diacetylene groups (Figure 1B). These formulations, as demonstrated earlier, are not susceptible to 514 nm laser treatments, and hence a direct role of lipid oxidation in our systems seems an unlikely explanation. Therefore, we next considered the requirement of photoactivated Cal-G for observed release. The findings described below support our hypothesis.

First, we used AA, a naturally occurring molecule with antioxidant properties that affect both type I and type II photoactivation pathways.[36] Liposomes were treated with the 514 nm laser in the presence or absence of AA (0–1 mM). Incubation of AA (0.5–1.0 mM, 24 hours at 25°C) with Cal-G-loaded DPPC:$DC_{8,9}PC$ liposomes (formulation I, containing ≈1.5 nmol Pi/mL in 0.1–0.2 mL) resulted in a dramatic reduction of 514 nm laser-triggered Cal-G release from 35%–40% to less than 15% (Figure 4A). In contrast, the extent of Cal-G release remained unaffected even in the presence of AA when samples were exposed to UV (254 nm) light for 30 minutes at room temperature (data not shown). To further substantiate these inhibitory effects, the AA consumption in the 514 nm laser-treated samples was determined by measuring the absorbance of AA at 265 nm (Figure 4A). It is clear that AA concentration was only reduced upon 514 nm laser treatment when Cal-G-loaded liposomes were used (Figure 4A). A decrease in AA concentration was not observed when either Cal-B-loaded or empty liposomes were tested (Figure 4A). A direct analysis of the effect of 514 nm laser treatment on AA consumption in the presence of free photo-agents is also shown in Figure 4A. AA was added to free Cal-G or Cal-B (as equivalent concentrations of liposome-entrapped Cal-G or Cal-B), and absorbance was measured. Therefore, the 514 nm/Cal-G combination but not the 514 nm/Cal-B combination resulted in decrease of AA consumption, suggesting photo-agent-specific effects. The data presented here suggest that oxygen radicals play a role in 514 nm laser-triggered release mechanisms from Cal-G-loaded liposomes (formulations I or IV).

Sodium azide, a singlet oxygen scavenger, does not block 514 nm laser-mediated Cal-G release from liposomes

The results presented in the previous section demonstrated that (1) our payload release from the photo-triggerable formulations involves ROS, and (2) that the ROS production is dependent on the light-induced activation of the entrapped solute in a wavelength-specific manner, in agreement with the characteristic of the photo-agent. To further identify the dominant ROS species, we used NaN_3, a singlet oxygen scavenger that would block the type II pathway.[37,38] Thus, NaN_3 at 10 mM concentration was coencapsulated with Cal-G in the interior of the DPPC:$DC_{8,9}PC$ liposomes (formulation I), and Cal-G release was monitored. The results presented in Figure 4B show that inclusion of NaN_3 in formulation I failed to mitigate/block 514 nm laser-mediated Cal-G release. Based on these observations, we conclude that solute-release mechanisms from our photo-triggerable formulations primarily involve a type I photoactivation reaction.

Laser treatment of 514 nm of liposomes results in production of H_2O_2

Typically, the type I photo-activated pathway is associated with the production of H_2O_2 as one of the end products. Therefore, we determined the production levels of H_2O_2 in 514 nm laser-treated liposomes. Liposomes containing encapsulated Cal-G (formulation I, Table 1) or Cal-B

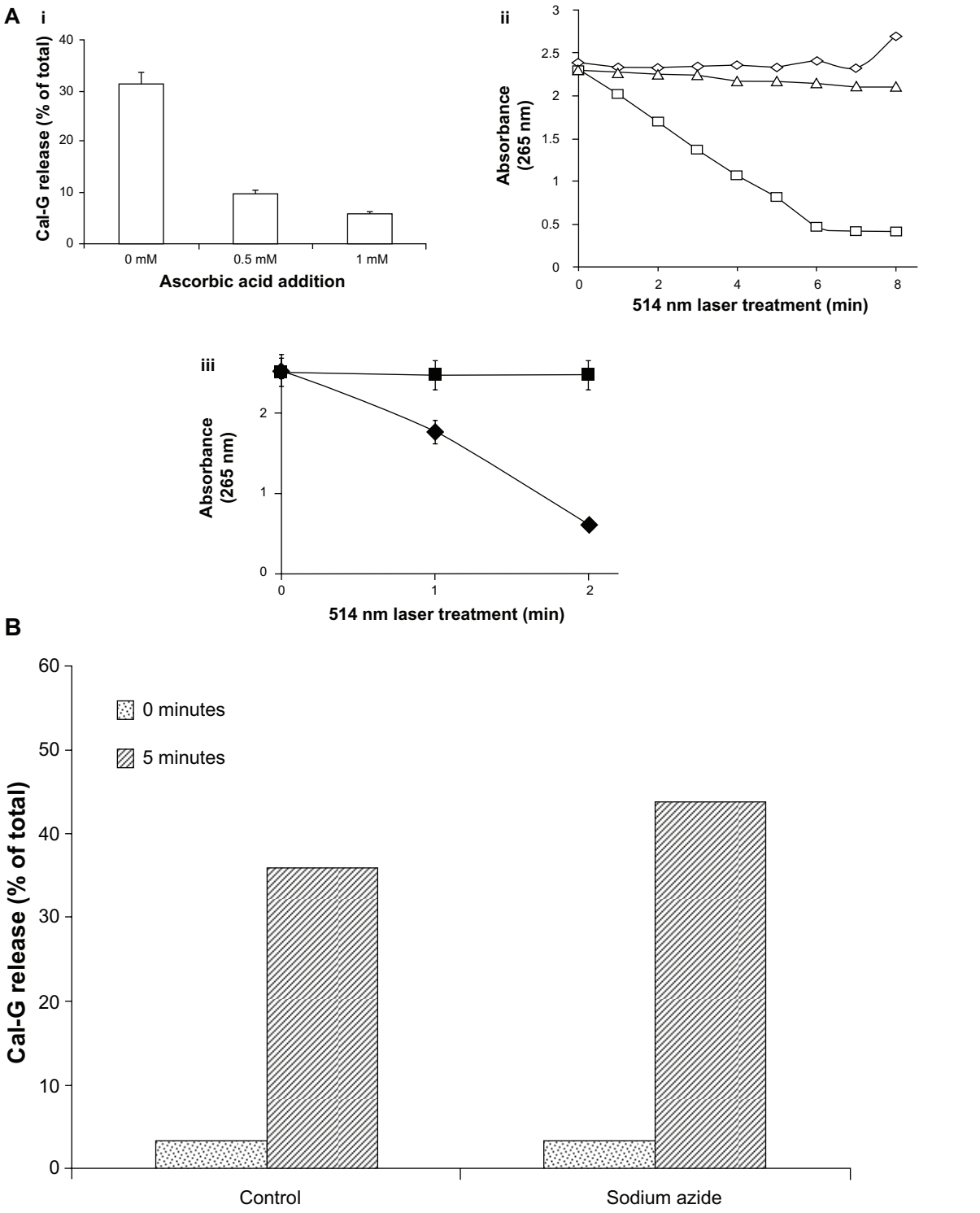

Figure 4 (**A**) Effect of ascorbic acid (AA) on 514 nm laser-triggered calcein green (Cal-G) release from formulation I. (i): AA inhibits 514 nm laser-triggered Cal-G release from liposomes. AA (0, 0.5, or 1 mM) was added to the Cal-G loaded liposomes (formulation I, Table 1) for 24 hours at room temperature and then exposed to 514 nm laser, and Cal-G release from liposomes was measured (Materials and methods section). The values are expressed as percentage of Cal-G release from liposomes taking triton X (TX)-100 fluorescence as 100% leakage. (ii): AA consumption in 514 nm laser-treated liposomes. AA (0.625 mM) was added to Cal-G (formulation I, squares) or calcein blue (Cal-B; formulation II, triangles). Subsequently, liposomes were treated by 514 nm laser for 0–8 minutes and degradation of AA was detected by absorbance measurement (265 nm). Empty liposomes (without encapsulation of calcein, diamonds) were used as controls. (iii): Effect of free dyes on AA consumption. AA (0.625 mM) was added to Cal-G (diamonds) or Cal-B (squares). After treatment by 514 nm laser for 0–3 minutes, AA degradation was detected by absorbance measurement at 265 nm. (**B**) Effect of NaN_3 on 514 nm laser-triggered calcein release from liposomes. NaN_3 was encapsulated within liposomes (formulation I) during sonication at a concentration of 10 mM. The percentage of calcein released in NaN_3 coencapsulated and control liposomes before (dotted bar) and after treatment (diagonal bars) with a 514 nm laser (5 minutes) was detected by fluorescence measurement.

(formulation II, Table 1) were treated with the 514 nm laser for 5 minutes, and H_2O_2 levels were measured in the samples using the Amplex red assay. Untreated samples were used as controls as indicated, and the findings are presented in Figure 5A. The 514 nm laser treatment of formulation I (containing Cal-G) resulted in a significantly high production of H_2O_2 concentration levels (≈100 μM), well above the background levels (<10 μM; Figure 5A, formulation I); liposomes that were not treated with 514 nm laser did not yield any measurable H_2O_2 above the background levels under identical conditions (Figure 5A). Moreover, the 514 nm laser-exposed Cal B-loaded liposomes (formulation II) did not result in production of H_2O_2 under identical experimental conditions. The results are reproducible from two independent experiments. These data support our hypothesis that laser-triggered release occurs primarily via a type I photoactivation mechanism.

We also conducted separate experiments to elucidate the consequence of direct H_2O_2 interactions (in the absence of laser treatments) with our DPPC:$DC_{8,9}PC$ liposomes (formulation I) and potential effects on Cal-G release. These studies entailed direct addition of H_2O_2 to our Cal-G loaded liposomes. We utilized concentrations of H_2O_2 that did not cause photo-bleaching of Cal-G, and performed the studies with final concentrations of H_2O_2 ranging from 0 to 1 mM without any green laser-light exposure. Liposomes were incubated with H_2O_2 at room temperature for up to 40 minutes and Cal-G release was monitored. The results following 40 minutes incubation with H_2O_2 are shown in Figure 5B. It is clear that H_2O_2 addition had no effect on the release of Cal-G above the background levels (Figure 5B). Since high levels of H_2O_2 alone (up to 1 mM) did not cause release of Cal-G, photoactivation of Cal-G is required for its release from the photo-triggerable liposomes (formulation I).

$K_3Fe(CN)_6$, an electron-transfer agent, inhibits Cal-G release from photo-triggerable formulation I

The data presented and the lack of $DC_{8,9}PC$ photo-cross-linking upon 514 nm laser treatment (Figure 2) led us to consider the possibility of indirect photo-induced reversible modifications in $DC_{8,9}PC$ (within the DPPC matrix), which could be mediated through the photoactivated state of Cal-G. As in other known type I photoreactions with a photo-agent, photoactivated Cal-G is hypothesized to donate an electron to the $DC_{8,9}PC$ lipids, resulting in reversible kink formations of the $DC_{8,9}PC$ fatty acyl chains, leading to liposome-membrane perturbations. Although a detailed analysis of structural modifications in the lipid molecules (and possibly photoactivated Cal-G) upon light treatments is desirable, such analyses are subject to future investigations. In order to gain insight into the involvement of this mechanistic possibility of Cal-G release from formulation I, we utilized $K_3Fe(CN)_6$, a known electron acceptor.[39,40] Liposomes were prepared in the presence or absence of $K_3Fe(CN)_6$ (100 mM). The liposomes were treated with the green (514 nm) laser light, and the efflux of Cal-G release was monitored. The data presented in Figure 6 show substantial reduction in the levels of Cal-G

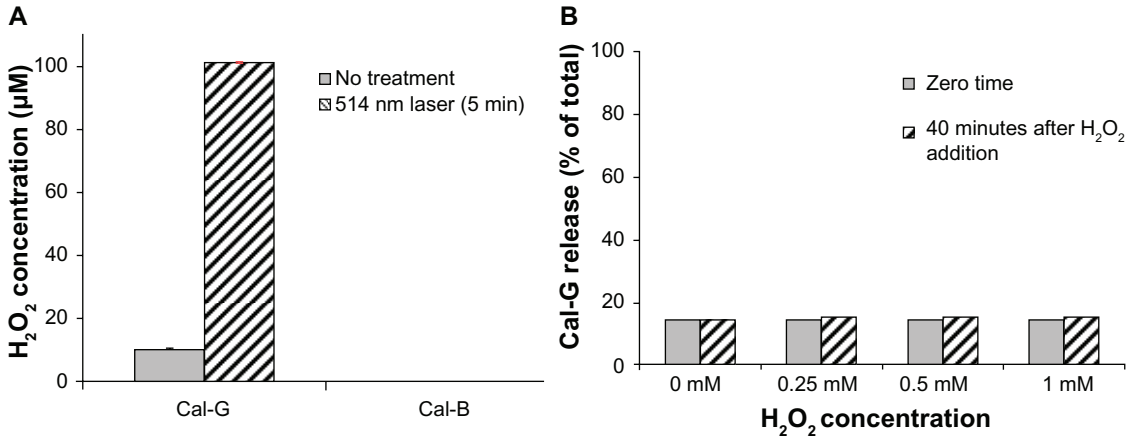

Figure 5 (**A**) Production of H_2O_2 in 514 nm laser-treated liposomes. Calcein-loaded liposomes (formulations I and II) were treated by 514 nm laser (5 minutes) and filtered, and H_2O_2 concentration was measured, as described in the Materials and methods section. Standard deviation values were as follows: calcein green (Cal-G), 0.177 and 0.13 μM before and after laser treatment, respectively; calcein blue (Cal-B), 0.425 and 0.016 μM before and after laser treatment, respectively. (**B**) Direct addition of H_2O_2 does not rupture liposomes in the absence of light. H_2O_2 (0–1 mM) was added directly to Cal-G-loaded liposomes (formulation I), and samples were allowed to incubate at room temperature (25°C) for 0–40 minutes. Cal-G release was measured (Materials and methods section). Fluorescence was then measured to determine if liposomes had released calcein. Triton X-100 (10 μL) was then added to each sample, and fluorescence was measured again to serve as a comparison of total release. Solid-gray bars, time zero; diagonal bars, liposomes incubated for 40 minutes. Standard deviation values at various concentrations of H_2O_2 were as follows: time zero, 0.35 (0 mM), 0.005 (0.25 mM), 0.026 (0.5 mM), and 0.098 (1 mM); 40-minute incubations, 0.18 (0 mM), 0.055 (0.25 mM), 0.054 (0.5 mM), and 0.031 (1 mM).

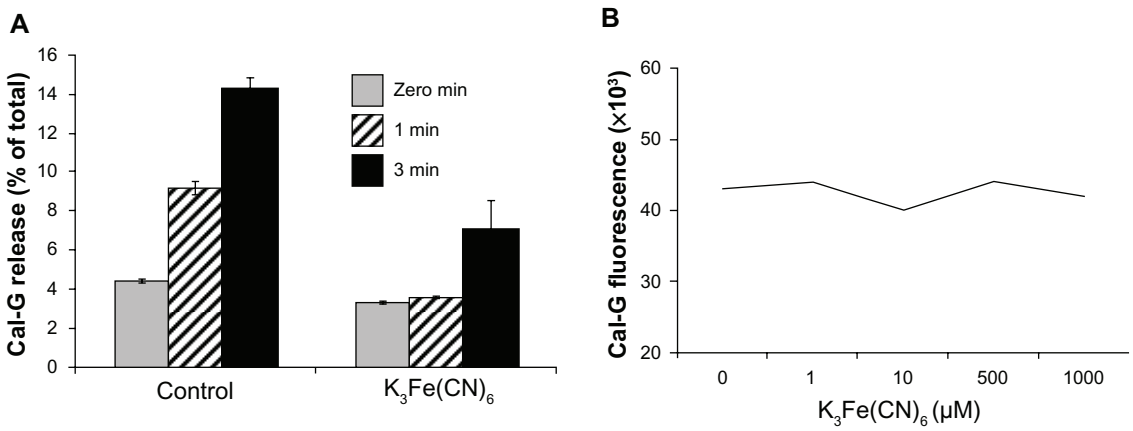

Figure 6 (**A** and **B**) Effect of potassium ferricyanide on calcein green (Cal-G) release from liposomes. Liposomes were prepared using the lipid composition dipalmitoylphosphatidylcholine (DPPC):1,2-bis (tricosa-10,12-diynoyl)-*sn*-glycero-3-phosphocholine ($DC_{8,9}PC$): distearoylphosphatidylethanolamine (DSPE)-polyethylene glycol (PEG)-2000 (88:10:02 mol%) and were loaded with Cal-G alone or Cal-G and $K_3Fe(CN)_6$ (see Materials and methods section for details). Liposomes were treated with 514 nm laser for 0–3 minutes, and Cal-G release was monitored (expressed as percentage of total, **A**). Solid grey, 0-minute; diagonal bars, 1-minute; solid black bars 3-minute laser treatments. Fluorescence of free Cal-G was also tested in the presence of various concentrations of $K_3Fe(CN)_6$ (**B**).

release when formulation I coencapsulated with $K_3Fe(CN)_6$ was tested.(Figure 6A). Free $K_3Fe(CN)_6$ has no direct influence on Cal-G fluorescence, thus enabling accurate Cal-G-release measurements (Figure 6B).

Proposed mechanisms for 514 nm laser-enhanced DPPC:$DC_{8,9}PC$ liposome permeabilization

Some photo-agents possess a metastable state in which the excited photo-agent is "long-lived" (10^{-3} to 1 seconds, in contrast to the excited- to ground-state lifetime transition through the process of fluorescence of ~10^{-8} seconds). Due to the fact that the spin of the photon is zero, the spin of the electron is conserved during the quantum transition. Consequently, upon photon absorption, the photo-agent Cal-G makes a transition from its singlet ground state, ^1P, to its excited singlet state, $^1P^*$ (see Figure 7). If during the time course of the photo-agent's excited state lifespan, the excited electron flips its spin, the photo-agent makes a transition from the singlet excited state into its triplet excited state, $^3P^*$. Since the transition of the excited electron from its triplet excited state back to the molecule's singlet ground state is forbidden through Pauli's

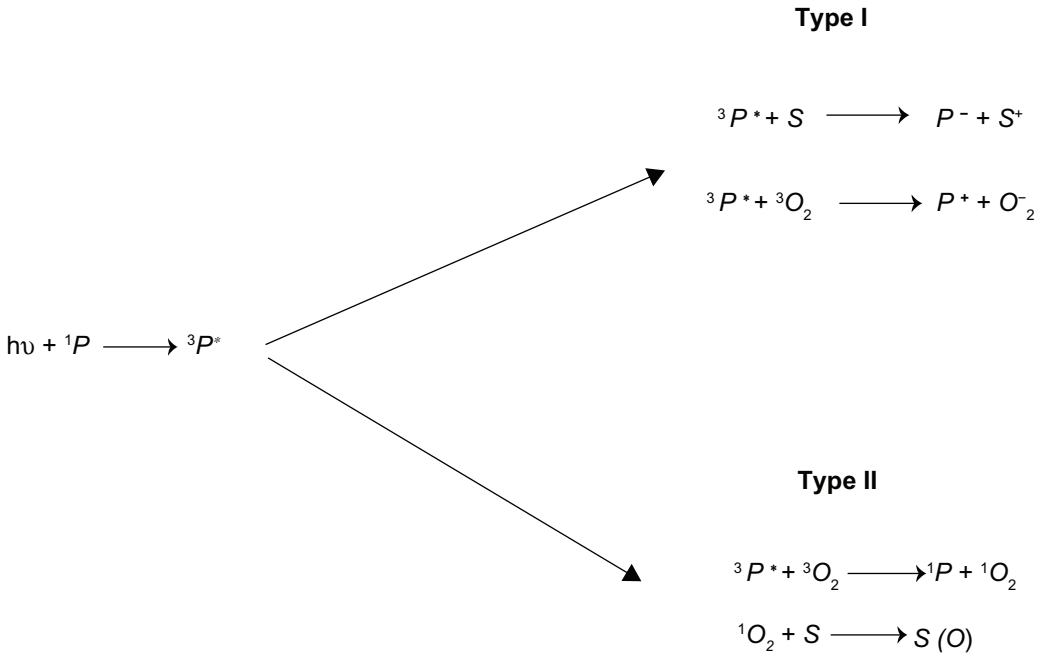

Figure 7 Schematic presentation of the photoactivation reactions.

exclusion principle, the photo-agent molecule remains excited for a long duration in which opportunistic interactions can occur between the excited photo-agent and its surrounding environment.

Two mechanistic pathways of interactions are plausible. In the type I pathway, the excited photo-agent Cal-G either transfers its excited electron to substrate S (such as in our consideration lipid moieties) or to molecular oxygen-forming superoxide anions – O_2^-.The O_2^- in turn, with a rapid combination with two-proton dismutase, yields to long-lived H_2O_2 (Figure 7). As noted, our experimental findings indeed confirm the generation of H_2O_2 due to the 514 nm laser-activated (liposome-entrapped) Cal-G (Figure 5), thus confirming the presence of type I mechanistic processes. However, as noted in the separate parallel experiments without the laser irradiation, that addition of copious levels of exogenous H_2O_2 to the DPPC:$DC_{8,9}$PC liposomes did not result in any enhanced Cal-G release, thus leading us to rule out H_2O_2 as the key player in the permeabilization of the liposome membrane. In a type II pathway the excited photo-agent Cal-G is expected to transfer its excited energy onto the ground (triplet) state, $^3O_2$, resulting in an excited oxygen molecule in its singlet state $^1O_2$. However, as noted above, our singlet oxygen-scavenger studies have revealed that singlet oxygen is not a key player responsible for the enhanced permeabilization of the liposome lipid membrane. This leads us to three other remaining possibilities: 1) the direct interaction of the lipids with the superoxide anion O_2^- through type I processes, 2) direct interaction of Cal-G in its excited triplet state, with the lipid bilayer molecules resulting in charge transfer to or from the lipids, or 3) same mechanistic processes as in the type II pathway, except here the molecular oxygen is now replaced with the lipid molecule, ie, direct Cal-G triplet state energy transfer can be envisioned to occur onto the triple carbon bonds, resulting in reversible kink formation of the fatty acyl chains and thus enhanced liposome-membrane permeability. These three possibilities are consistent with our AA findings, in which the AA molecule is viewed to compete with the lipid molecule for the O_2^-, as well as for the excited triplet state energy donation from the Cal-G molecule.

Conclusion

Photoactivatable lipids have long been sought as the building blocks of nanocarriers such as liposomes to deliver pharmaceutical payloads. In the field of cancer nanomedicine, photo-triggering is one avenue for improved delivery of the drugs or bioactive molecules. In this study, we investigated the mechanism responsible for the 514 nm laser-triggered release of the Cal-G payload through the inhibitory actions of several scavengers that are known to specifically inhibit either type I or type II photoreaction pathways. We deduce through our scavenger studies that the 514 nm laser-triggered release of Cal-G from the photo-triggerable DPPC:$DC_{8,9}$PC:DSPE-PEG2000 liposome formulation predominately involves a photoactivated Cal-G and primarily occurs through a type I photoreaction pathway.

Acknowledgments

This project was funded in whole or in part with federal funds from the National Cancer Institute, National Institutes of Health, under contract number HHSN261200800001E. The content of this publication does not necessarily reflect the views or policies of the Department of Health and Human Services, nor does mention of trade names, commercial products, or organizations imply endorsement by the US Government. This research was supported (in part) by the Intramural Research Program of the NIH, National Cancer Institute, Center for Cancer Research. We thank Alex Haber and Christopher Connor for their help with the experiments.

Disclosure

The authors report no conflicts of interest in this work. The mention of commercial products, their sources, or their use in connection with material reported herein is not to be construed as either an actual or implied endorsement of such products by the US Department of Health and Human Services.

References

1. Jin CS, Zheng G. Liposomal nanostructures for photosensitizer delivery. *Lasers Surg Med.* 2011;43:734–748.
2. Juarranz A, Jaen P, Sanz-Rodriguez F, Cuevas J, Gonzalez S. Photodynamic therapy of cancer. Basic principles and applications. *Clin Transl Oncol*. 2008;10:148–154.
3. Nawalany K, Rusin A, Kepczynski M, et al. Novel nanostructural photosensitizers for photodynamic therapy: in vitro studies. *Int J Pharm.* 2012;430:129–140.
4. Séguier S, Souza SL, Sverzut AC, et al. Impact of photodynamic therapy on inflammatory cells during human chronic periodontitis. *J Photochem Photobiol B*. 2010;101:348–354.
5. Bisby RH, Mead C, Morgan CG. Wavelength-programmed solute release from photosensitive liposomes. *Biochem Biophys Res Commun.* 2000;276:169–173.
6. Clapp PJ, Armitage BA, Obrien DF. Two-dimensional polymerization of lipid bilayers: visible-light-sensitized photoinitiation. *Macromolecules*. 1997;30:32–41.
7. Lamparski H, Liman U, Barry JA, et al. Photoinduced destabilization of liposomes. *Biochemistry*. 1992;31:685–694.
8. Lasic DD, Bolotin E, Brey RN. Polymerized liposomes: from biophysics to applications. Part I. *Chim Oggi.* 2000;18:48–51.
9. Shum P, Kim JM, Thompson DH. Phototriggering of liposomal drug delivery systems. *Adv Drug Deliv Rev.* 2001;53:273–284.

10. Yavlovich A, Singh A, Tarasov S, Capala J, Blumenthal R, Puri A. Design of liposomes containing photopolymerizable phospholipids for triggered release of contents. *J Therm Anal Calorim.* 2009;98:97–104.
11. Yavlovich A, Smith B, Gupta K, Blumenthal R, Puri A. Light-sensitive lipid-based nanoparticles for drug delivery: design principles and future considerations for biological applications. *Mol Membr Biol.* 2010;27:364–381.
12. Chandra B, Mallik S, Srivastava DK. Design of photocleavable lipids and their application in liposomal "uncorking." *Chem Commun (Camb)*. 2005;3021–3023.
13. Bisby RH, Mead C, Mitchell AC, Morgan CG. Fast laser-induced solute release from liposomes sensitized with photochromic lipid: effects of temperature, lipid host, and sensitizer concentration. *Biochem Biophys Res Commun.* 1999;262:406–410.
14. Yavlovich A, Singh A, Blumenthal R, Puri A. A novel class of photo-triggerable liposomes containing DPPC:DC(8,9)PC as vehicles for delivery of doxorubicin to cells. *Biochim Biophys Acta*. 2011;1808: 117–126.
15. Puri A, Blumenthal R. Polymeric lipid assemblies as novel theranostic tools. *Acc Chem Res.* 2011;44:1071–1079.
16. Fomina N, McFearin C, Sermsakdi M, Edigin O, Almutairi A. UV and near-IR triggered release from polymeric nanoparticles. *J Am Chem Soc.* 2010;132:9540–9542.
17. Fomina N, Sankaranarayanan J, Almutairi A. Photochemical mechanisms of light-triggered release from nanocarriers. *Adv Drug Deliv Rev.* 2012;64:1005–1020.
18. Leung SJ, Romanowski M. Light-activated content release from liposomes. *Theranostics.* 2012;2:1020–1036.
19. Henderson BW, Dougherty TJ. How does photodynamic therapy work? *Photochem Photobiol.* 1992;55:145–157.
20. Puri A, Jang H, Yavlovich A, et al. Material properties of matrix lipids determine the conformation and intermolecular reactivity of diacetylenic phosphatidylcholine in the lipid bilayer. *Langmuir*. 2011;27: 15120–15128.
21. Ames BN, Dubin DN. The role of polyamines in the neutralization of bacteriophage deoxyribonucleic acid. *J Biol Chem.* 1960;235: 769–775.
22. Raviv Y, Viard M, Bess J Jr, Blumenthal R. Quantitative measurement of fusion of HIV-1 and SIV with cultured cells using photosensitized labeling. *Virology*. 2002;293:243–251.
23. Johnston DS, McLean LR, Whittam MA, Clark AD, Chapman D. Spectra and physical properties of liposomes and monolayers of polymerizable phospholipids containing diacetylene groups in one or both acyl chains. *Biochemistry*. 1983;22:3194–3202.
24. Pons M, Johnston DS, Chapman D. The optical activity and circular dichroic spectra of diacetylenic phospholipid polymers. *Biochim Biophys Acta*. 1982;693:461–465.
25. Regen SL, Singh A, Oehme G, Singh M. Polymerized phosphatidyl choline vesicles. Stabilized and controllable time-release carriers. *Biochem Biophys Res Commun.* 1981;101:131–136.
26. Rhodes DG, Blechner SL, Yager P, Schoen PE. Structure of polymerizable lipid bilayers. I – 1,2-Bis(10,12-tricosadiynoyl)-sn-glycero-3-phosphocholine, a tubule-forming phosphatidylcholine. *Chem Phys Lipids*. 1988;49:39–47.
27. Schnur JM, Ratna BR, Selinger JV, Singh A, Jyothi G, Easwaran KRK. Diacetylenic lipid tubules – experimental-evidence for a chiral molecular architecture. *Science*. 1994;264:945–947.
28. Blumenthal R, Ralston E, Dragsten P, Leserman LD, Weinstein JN. Lipid vesicle-cell interactions: analysis of a model for transfer of contents from adsorbed vesicles to cells. *Membr Biochem.* 1982;4:283–303.
29. Blumenthal R, Henkart M, Steer CJ. Clathrin-induced pH-dependent fusion of phosphatidylcholine vesicles. *J Biol Chem.* 1983;258:3409–3415.
30. Stratford RE Jr, Yang DC, Redell MA, Lee VH. Ocular distribution of liposome-encapsulated epinephrine and inulin in the albino rabbit. *Curr Eye Res.* 1982;2:377–386.
31. Girotti AW. Mechanisms of photosensitization. *Photochem Photobiol.* 1983;38:745–751.
32. Girotti AW. Photodynamic lipid peroxidation in biological systems. *Photochem Photobiol.* 1990;51:497–509.
33. Girotti AW. Lipid hydroperoxide generation, turnover, and effector action in biological systems. *J Lipid Res.* 1998;39:1529–1542.
34. Pratt DA, Tallman KA, Porter NA. Free radical oxidation of polyunsaturated lipids: new mechanistic insights and the development of peroxyl radical clocks. *Acc Chem Res.* 2011;44:458–467.
35. Frankel EN. Lipid oxidation. *Prog Lipid Res.* 1980;19:1–22.
36. Bodannes RS, Chan PC. Ascorbic acid as a scavenger of singlet oxygen. *FEBS Lett.* 1979;105:195–196.
37. Franco R, Panayiotidis MI, Cidlowski JA. Glutathione depletion is necessary for apoptosis in lymphoid cells independent of reactive oxygen species formation. *J Biol Chem.* 2007;282:30452–30465.
38. Tyrrell RM, Pidoux M. Singlet oxygen involvement in the inactivation of cultured human fibroblasts by UVA (334 nm, 365 nm) and near-visible (405 nm) radiations. *Photochem Photobiol.* 1989;49:407–412.
39. Estabrook RW. Studies of oxidative phosphorylation with potassium ferricyanide as electron acceptor. *J Biol Chem.* 1961;236:3051–3057.
40. Runquist JA, Loach PA. Catalysis of electron transfer across phospholipid bilayers by iron-porphyrin complexes. *Biochim Biophys Acta*. 1981;637:231–244.

International Journal of Nanomedicine Dovepress

Publish your work in this journal

The International Journal of Nanomedicine is an international, peer-reviewed journal focusing on the application of nanotechnology in diagnostics, therapeutics, and drug delivery systems throughout the biomedical field. This journal is indexed on PubMed Central, MedLine, CAS, SciSearch®, Current Contents®/Clinical Medicine, Journal Citation Reports/Science Edition, EMBase, Scopus and the Elsevier Bibliographic databases. The manuscript management system is completely online and includes a very quick and fair peer-review system, which is all easy to use. Visit http://www.dovepress.com/testimonials.php to read real quotes from published authors.

Submit your manuscript here: http://www.dovepress.com/international-journal-of-nanomedicine-journal